

Nonlinear Transport through Quantum Dots Studied by the Time-Dependent DMRG

Shunsuke Kirino* and Kazuo Ueda

The Institute for Solid State Physics, The University of Tokyo, Kashiwanoha 5-1-5, Kashiwa, Chiba 277-8581 Japan

Key words quantum dot, Kondo effect, transport, nonequilibrium, time-dependent DMRG

Recent developments on studies of transport through quantum dots obtained by applying the time-dependent density matrix renormalization group method are summarized. Some new aspects of Kondo physics which appear in nonequilibrium steady states are discussed both for the single dot case and for the serially coupled double-quantum-dot case.

Copyright line will be provided by the publisher

1 Introduction

Advancements in microfabrication technology provide us opportunities to investigate transport properties through quantum dots. Stimulated by possible application to quantum computation, number of interesting systems are now being produced by arranging multiple quantum dots in various geometries.

In the simplest case, namely a single quantum dot system, it was predicted [1] and experimentally observed [2] that the linear conductance is enhanced at low temperatures up to the unitary limit by the Kondo effect when odd number of electrons are accommodated in the dot.

To measure a current through quantum dots a finite bias voltage is applied between source and drain electrodes. Therefore, in principle, we always confront the problem of nonlinear transport. Away from the linear response regime, the differential conductance for single dot system is quickly suppressed reflecting the sharp Kondo resonance peak at the Fermi energy. The nonlinear transport through quantum dots defines a prototypical problem for electron correlation under a nonequilibrium condition. Various theoretical approaches have been applied to this problem but our understanding of the problem is still far from complete. Therefore it is desirable to obtain unbiased results by using some computational approaches.

Recently there has been progress in computational physics for strongly correlated electron systems from two complementary approaches. One is from the infinite dimension initiated by Metzner and Vollhardt [3], which was later developed into the dynamical mean field theory (DMFT) [4]. It is interesting to note that the Kondo effect is relevant to the DMFT since in the infinite dimension the self-energy becomes local, which is determined by similar physics as the Kondo effect. The other is the density matrix renormalization group method developed by White [5], which is an approach from one dimension. Among many numerical techniques which have been extended to nonequilibrium situations, the time-dependent density matrix renormalization group method (TddMRG) [6] has proven to be a powerful tool to tackle the nonlinear transport in strongly correlated electron systems, such as the single quantum dot system [8, 9, 11, 10] and the interacting resonant level model [12, 13]. In this paper we discuss our recent activities to understand the nonequilibrium transport through quantum dots by using the TddMRG. We will briefly summarize our results concerning the single quantum dot [9, 11] and then show recent results on the serial double-dot system.

* Corresponding author E-mail: kirino@issp.u-tokyo.ac.jp, Phone: +81 471 363 272

2 Single Quantum Dot System

We consider a system consisting of a quantum dot and two leads. We focus on the situation where the level spacing in the quantum dot is large compared to the other energy scales in the system, so that only one level in the dot is active and the others are effectively frozen. Concerning the leads we assume that single channel is relevant to transport, which can be described by the 1-D tight-binding model. The Hamiltonian for the system is expressed as follows:

$$\begin{aligned}
H(\tau) = & -t \sum_{i < -1} \sum_{\sigma} (c_{i\sigma}^{\dagger} c_{i+1\sigma} + h.c.) - t \sum_{i > 0} \sum_{\sigma} (c_{i\sigma}^{\dagger} c_{i+1\sigma} + h.c.) \\
& - t' \sum_{\sigma} \left[(c_{-1\sigma}^{\dagger} c_{0\sigma} + h.c.) + (c_{0\sigma}^{\dagger} c_{1\sigma} + h.c.) \right] \\
& - \frac{U}{2} \sum_{\sigma} c_{0\sigma}^{\dagger} c_{0\sigma} + U c_{0\uparrow}^{\dagger} c_{0\downarrow}^{\dagger} c_{0\downarrow} c_{0\uparrow} + \frac{eV}{2} \theta(\tau) (N_L - N_R),
\end{aligned} \tag{1}$$

where τ is the time variable, the quantum dot is located at the 0th site and $c_{i\sigma}^{\dagger}$ creates an electron with spin σ at i th site. t, t', U and V are the hopping amplitude in leads, the one between the dot and the neighboring sites, the Coulomb repulsion energy and the voltage drop between the two leads, respectively. Here we assume the electron-hole symmetry, which means that the one-particle energy at the dot site is fixed as $-U/2$, and the inversion symmetry at the dot site except for the voltage term. N_L is the sum of the number operators in the left lead and N_R in the right lead. In the following we focus on the half-filled case.

In the Keldysh formalism, one starts with an equilibrium state of an unperturbed Hamiltonian. One then turns on the perturbation term adiabatically, and gets a nonequilibrium steady state after a relaxation time. Although there are several choices for dividing the Hamiltonian into unperturbed and perturbed terms, the nonequilibrium steady states for the full Hamiltonian are expected to be independent of the choice. For the present problem we take a time-dependent voltage term. $\theta(\tau)$ is a smoothed step function which is introduced to simulate adiabatic switching-on of the voltage. Throughout this paper we set $\theta(\tau)$ as

$$\theta(\tau) \equiv \frac{1}{\exp\left(\frac{\tau_0 - \tau}{\tau_1}\right) + 1}. \tag{2}$$

The reason for our choice of the time dependence of the Hamiltonian is that, if t' is chosen as the perturbation, there is only one nonzero eigenvalue of the reduced density matrix of the lead parts, i.e. the entanglement entropy between dot and leads are zero for the initial states. Then the usual DMRG scheme to obtain the optimal basis set, which will be necessary for the subsequent TdDMRG calculation, cannot be used directly.

By the TdDMRG method we can compute the time evolution of the initial wave function. In order to obtain the current at each time we can simply take the expectation values as follows:

$$J(\tau) = -\langle \psi(\tau) | e \dot{N}_L | \psi(\tau) \rangle = \frac{iet'}{\hbar} \sum_{\sigma} \langle \psi(\tau) | (c_{0\sigma}^{\dagger} c_{-1\sigma} - h.c.) | \psi(\tau) \rangle. \tag{3}$$

Note that one can define the current operators for every bond in the system. When the system reaches a steady state, the currents stay constant at a certain value because of the definition of the steady states and the charge conservation.

The steady current in the thermodynamic limit can be calculated based on the Keldysh formalism as [14]

$$J(V) = \frac{e}{\hbar} \sum_{\sigma} \int_{-\frac{eV}{2}}^{\frac{eV}{2}} d\omega \frac{\Gamma_L \Gamma_R}{\Gamma_L + \Gamma_R} \left(-\frac{1}{\pi} \right) \text{Im} (g_{\text{dot}}^r(\omega)), \tag{4}$$

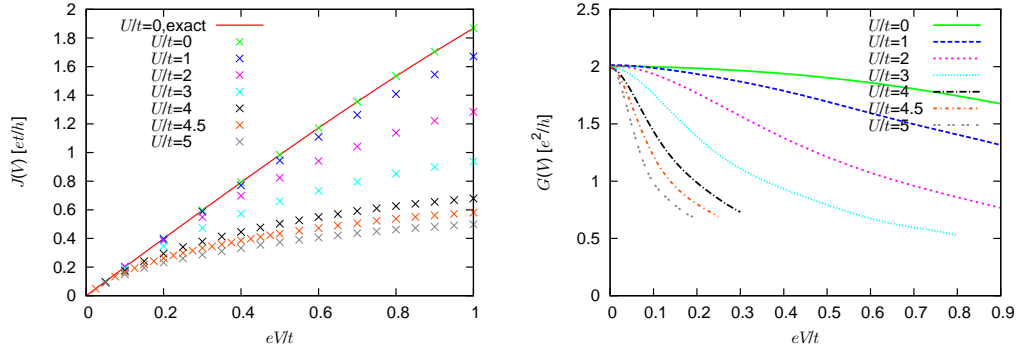


Fig. 1 (Left) Current-voltage characteristics of the Anderson model Eq.(1). (Right) Differential conductance obtained by interpolating $J(V)$. We omit the data where numerical differentiation is so delicate that it can produce an unphysical peak structure in $G(V)$. Adopted from Ref.[11].

where $\Gamma_{L,R}(\omega)$ is the resonance width due to the hybridization to the left and right leads which will be assumed to be the same in this paper, and $g_{\text{dot}}^r(\omega)$ the retarded Green's function at the dot site. When $U = 0$, the problem is simplified to the one-particle level. In this case Eq.(4) can be exactly evaluated. Alternatively, one can numerically diagonalize the one-particle Hamiltonian and explicitly calculate the time-evolution operator for a finite size system. Errors included in TdDMRG results can be estimated by comparing with results obtained from these methods.

Since our system is finite we cannot reach to real steady states. However, it is possible to evaluate steady currents from the quasi-steady states which are defined in the time domain after the initial relaxation time and before the arrival of the wave front reflected at the boundary of the system.

Quasi-steady states can be realized by the TdDMRG calculation for $U/t \leq 5$. The fixed value $t'/t = 0.6$ and the range for U correspond to the Wilson ratio $1 \leq R_W \leq 1.97$. Then we can extract the nonlinear current-voltage characteristics from the quasi-steady regions, which are summarized in Figs.1 [11]. In the noninteracting case the TdDMRG results perfectly agree with the exact analytic results for $L \rightarrow \infty$. Moreover, the linear conductance for every U corresponds to the prediction of the Fermi liquid theory [1],

$$\left. \frac{\partial J}{\partial V} \right|_{V=0} = \frac{2e^2}{h}. \quad (5)$$

In the differential conductance $G(V)$ we can see a substantial difference in the width of the zero bias peak depending on U which is a reflection of the sharp Kondo peak in the local density of states at the dot site. Therefore we can say that the TdDMRG calculation catches the essence of the Kondo effect of the quantum dot system out of equilibrium in the parameter space investigated.

3 Serial Double-Quantum-Dot System

Now we proceed to the serially coupled double-quantum-dot system [15, 16, 17, 18], each connected with a lead, and discuss transport properties in the system driven by a DC voltage. From a theoretical point of view the system can be modeled by the two impurity Anderson model.

The model is depicted in Fig.2 and it is straightforward to write the Hamiltonian explicitly in the similar form as Eq.(1). The only new additional parameter is the interdot hopping, $-t''$. In what follows we discuss the current between the two dots,

$$J(\tau) \equiv \frac{ie\tau''}{\hbar} \sum_{\sigma} \langle \psi(\tau) | (c_{r\sigma}^{\dagger} c_{l\sigma} - h.c.) | \psi(\tau) \rangle, \quad (6)$$

where $c_{l\sigma}^\dagger$ ($c_{r\sigma}^\dagger$) creates an electron at the left (right) dot.

There are several theoretical studies on the double-quantum-dot system. For the linear transport, the slave boson mean field theory (SBMFT) [19, 20] and the numerical renormalization group (NRG) method [21] have been applied to the problem and predicted that the linear conductance has a sharp peak which reaches the perfect conductance $2e^2/h$ as a function of the ratio of the interdot hopping amplitude t'' to the resonance width at the Fermi energy Γ , which is given by $\Gamma = t'^2/t$ for the present model. The peak is located at $J_{\text{eff}} \sim T_K^0$, where $J_{\text{eff}} = \frac{4t''^2}{U}$ denotes the antiferromagnetic exchange coupling between the two dots, and T_K^0 the Kondo temperature at $t'' = 0$.

This behavior can be understood in connection with formation and competition of the various types of singlets in the system as explained in Ref.[21]. The conductance formula is expressed by [22]

$$G = \frac{2e^2}{h} \sin^2(\delta_e - \delta_o), \quad (7)$$

where δ_e and δ_o are the scattering phase shifts for even and odd channels, respectively. The even and odd orbitals of the two dots are defined as $c_{e\sigma}^\dagger \equiv \frac{1}{\sqrt{2}}(c_{l\sigma}^\dagger + c_{r\sigma}^\dagger)$ and $c_{o\sigma}^\dagger \equiv \frac{1}{\sqrt{2}}(c_{l\sigma}^\dagger - c_{r\sigma}^\dagger)$. When each impurity site contains one electron, $\delta_e + \delta_o = \pi$ follows from the Friedel sum rule. Then, the following three characteristic states of the two impurity Anderson model appear depending on t'' , Γ and U :

- (i) For small t''/Γ such that $J_{\text{eff}} \ll T_K^0$, the Kondo singlet state is formed on each dot with its adjacent lead. The phase shifts for this state are $\delta_e \sim \delta_o \sim \pi/2$.
- (ii) In the intermediate t''/Γ region with $J_{\text{eff}} \gg T_K^0$, the local spins on both dots are coupled as a spin singlet state, $\frac{1}{\sqrt{2}}(c_{l\uparrow}^\dagger c_{r\downarrow}^\dagger - c_{l\downarrow}^\dagger c_{r\uparrow}^\dagger)|0\rangle$: a pair spin singlet. $\delta_e \sim \pi$, $\delta_o \sim 0$.
- (iii) When $t'' \gtrsim U/4$ the doubly occupied state of bonding orbital of the two dots, $c_{e\uparrow}^\dagger c_{e\downarrow}^\dagger|0\rangle$, becomes the most stable: a bonding singlet. $\delta_e \sim \pi$, $\delta_o \sim 0$.

The above three states are schematically shown in Fig.3 and their relationship is displayed in Fig.2 (b). For the ground state (i) the two dots are effectively decoupled and similarly for (ii) and (iii) the two dots

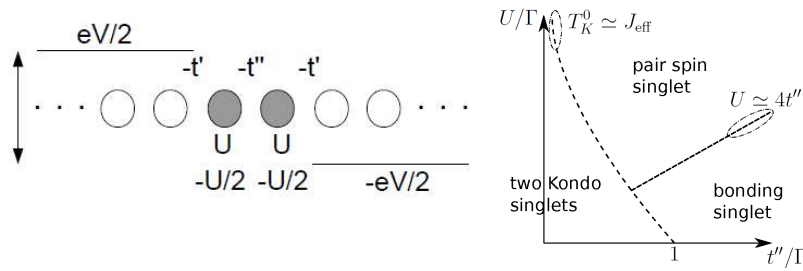


Fig. 2 (Left) Model of the serial double-quantum-dot system. (Right) Schematic diagram for the characteristic ground states (i), (ii) and (iii) on the $t'' - U$ plane. The curves represent crossover between the states.

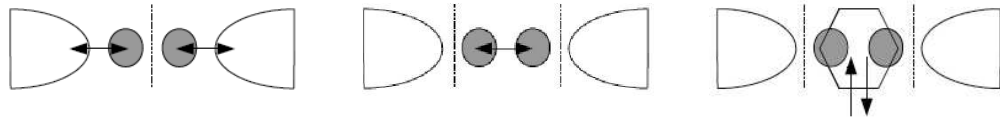


Fig. 3 (Left) Schematic figure of the two-Kondo-singlets state. (Middle) The pair spin singlet state. (Right) The bonding singlet state.

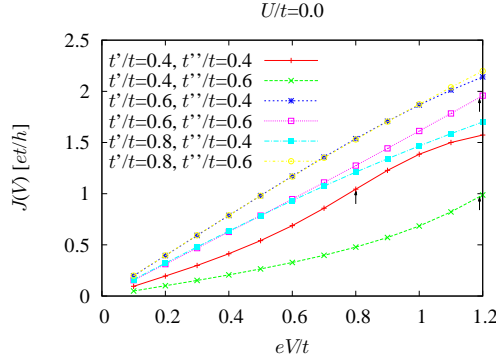


Fig. 4 Current-voltage characteristics of the serial double-quantum-dot system for $U = 0$ obtained by using exact diagonalization. Results for $t'/t = 0.6$ and $t''/t = 0.6$ are obtained for system of $L = 81$ sites and the others are for $L = 121$. Arrows indicate the positions of the inflection points, that is, the peak positions in the differential conductance $dJ(V)/dV$. Curves without associated arrows have inflection points at $V = 0$.

can be viewed as detached from the two leads, resulting in small conductance for all of the above states. A sharp peak with height $2e^2/h$ is found in the crossover region between (i) and (ii), namely $J_{\text{eff}} \approx T_K^0$. The continuous changes of δ_e and δ_o from (i) to (ii) (or directly to (iii) for relatively small U) with keeping the Friedel sum rule ensure that Eq.(7) has the maximum which reaches the perfect conductance. Just at the peak the system forms a coherent superposition of the two-Kondo singlets on the dots. As U increases or Γ decreases, in other words the electron correlation becomes strong, T_K^0 rapidly decreases and the peak position moves to smaller values of t'' . In addition the width of the peak becomes narrower, representing the decrease of the Kondo temperature. These intriguing behaviors can be attributed to the quasi-quantum criticality of the two impurity Kondo problem.

Let us first discuss the current-voltage characteristics in the noninteracting case. Since the parameters for the two dots are identical and the energy levels are set to be particle-hole symmetric, each dot contains exactly one electron. Then for $U = 0$ the linear conductance is given by

$$G = \frac{2e^2\Gamma^2}{h} |g_e(0+) - g_o(0+)|^2 = \frac{2e^2}{h} \frac{4(t''/\Gamma)^2}{[1 + (t''/\Gamma)^2]^2}. \quad (8)$$

G becomes the perfect conductance $2e^2/h$ at the point $t''/\Gamma = 1$. From Fig.4, the linear conductance for $(t'/t, t''/t) = (0.6, 0.4)$ and $(0.8, 0.6)$ is almost the perfect one ($1.98e^2/h$ and $1.99e^2/h$), since $t''/\Gamma = 1.11, 0.94$ is close to unity.

The LDOS for the even and odd states have peaks at $\pm t''$ with widths $\sim \Gamma$. The electrons moving through the two quantum dots, which are inside the bias window $-eV/2 \leq \omega \leq eV/2$, use these peaks in the resonant tunneling. When Γ is large, the two peaks merge into a single peak located at $\omega = 0$. On the other hand for $t'' > \Gamma$, the differential conductance $G(V) = \frac{\partial J(V)}{\partial V}$ has its maximum when the peaks in the LDOS come into the bias window. Concerning the results shown in Fig.4, for $t'/t = 0.6$ and 0.8 the maximum of the slope of $J(V)$ is located at $V = 0$, reflecting the single peak structure of the LDOS. On the other hand for $t'/t = 0.4$ we observe the split peaks of $G(V)$ at $eV = \pm 2t''$.

Now we consider the effects of the Coulomb interaction on the currents. First we study the linear conductance and it is summarized in Fig.5. For each U the conductance as a function of t''/Γ forms a peak near $t''/\Gamma = 1$ and their heights reach almost $2e^2/h$ [8, 19, 20, 21]. While on the right side of the peak the conductance decreases as U increases, it increases on the left side, reflecting the shift of the peak toward smaller t''/Γ , in accordance with the NRG results [21].

Several typical examples of the nonlinear currents of the double-quantum-dot system are shown in Fig.6 [23], together with the differential conductance $G(V) \equiv \frac{\partial J(V)}{\partial V}$ and the expectation values of the

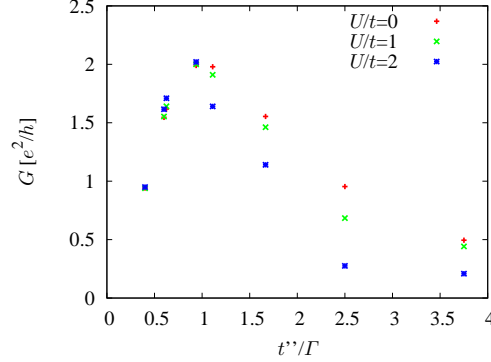


Fig. 5 Linear conductance of the serially coupled double-quantum-dot system obtained from $J(V)/V|_{eV/t=0.1}$. The sets of data are for $(t'/t, t''/t) = (1, 0.4), (1, 0.6), (0.8, 0.4), (0.8, 0.6), (0.6, 0.4), (0.6, 0.6), (0.4, 0.4)$ and $(0.4, 0.6)$ from left to right.

spin correlation operator $\langle \vec{S}_l \cdot \vec{S}_r \rangle$. Note that the results for $G(V)$ have larger errors than the others since they are obtained via interpolation and differentiation of the data points of $J(V)$.

The results for $(t'/t, t''/t) = (0.8, 0.6)$, not shown in this paper [23], are close to the linear conductance peak at $t''/\Gamma \simeq 1$. The linear conductance is thus near $2e^2/h$ and the system as a whole forms a coherent singlet state. Out of the linear response regime we find a substantial decrease of the current due to the Coulomb interaction. This can be attributed to the coherent singlet state whose weight of the LDOS builds up in a narrow region around the Fermi energy, similarly to the case of the single dot.

Next we discuss the results on the right side of the linear conductance peak at $t''/\Gamma \simeq 1$, that is, the results for $(t'/t, t''/t) = (0.4, 0.6)$, left panels in Fig.6. In this case the ground state has large amplitudes on the states (ii) and (iii), which can be confirmed by relatively large values of $|\langle \vec{S}_l \cdot \vec{S}_r \rangle|$. The splitting of the zero bias peak can be seen in $G(V)$ in this case. The position of the peak eV_{peak} moves to smaller V as increasing U and corresponds to the position where $|\langle \vec{S}_l \cdot \vec{S}_r \rangle|$ varies significantly. This can be explained as follows: as V becomes comparable to V_{peak} the local electronic state is modified in the steady state. Hence it is confirmed that the many-body bonding and antibonding states are located at $\pm eV_{\text{peak}}/2$ in the LDOS. This allows us to interpret $eV_{\text{peak}}/2$ as the effective hopping parameter $\tilde{t}''(U)$. Our results indicate that $\tilde{t}''(U)$ decreases by the renormalization effect due to the interaction. This simple picture qualitatively agrees with the SBMFT and the NCA results where the split peaks are located at $eV \ll t''$. For $(U/t, t'/t, t''/t) = (1, 0.6, 0.6)$ and $(2, 0.6, 0.6)$, not shown in this paper, the splitting cannot be seen since the relatively large resonance width Γ merges the two peaks at $\pm \tilde{t}''(U)$ into a single peak.

The SBMFT and the NCA results are for a fixed energy level in each dot and in the limit $U \rightarrow \infty$. If we consider the limit of $U \rightarrow \infty$ with keeping the particle-hole symmetry, we end up with the state (ii), since $T_K^0 \ll J_{\text{eff}}$ and $t'' \ll U/4$ always hold. There the pair spin singlet state is frozen and little current can flow. Thus, judging from our results we expect that the peak position moves toward $V = 0$ and, at the same time, the current is strongly suppressed by increasing U .

Now we turn to the left side of the linear conductance peak. $G(V)$ for $(t'/t, t''/t) = (0.8, 0.4)$ shows the zero bias peak, Fig.6 right panels. The width of the zero bias peak becomes narrow as increasing U , reflecting the formation of the sharp Kondo resonant peak. This behavior is basically the same as in the case of the single quantum dot system. In the parameter sets considered here, Γ is relatively large and therefore we see a broad linear response regime. A notable feature in this case is the enhancement of the spin correlation function $\langle \vec{S}_l \cdot \vec{S}_r \rangle$ by the finite bias voltage. The antiferromagnetic spin correlation in the steady states turn out to be enhanced compared with the ground state expectation values. Note that the states we are focusing on are near the two-Kondo singlet regime (the state (i)) and the spin correlation is small since the interdot correlation is effectively suppressed. By forcing the current flow through the double

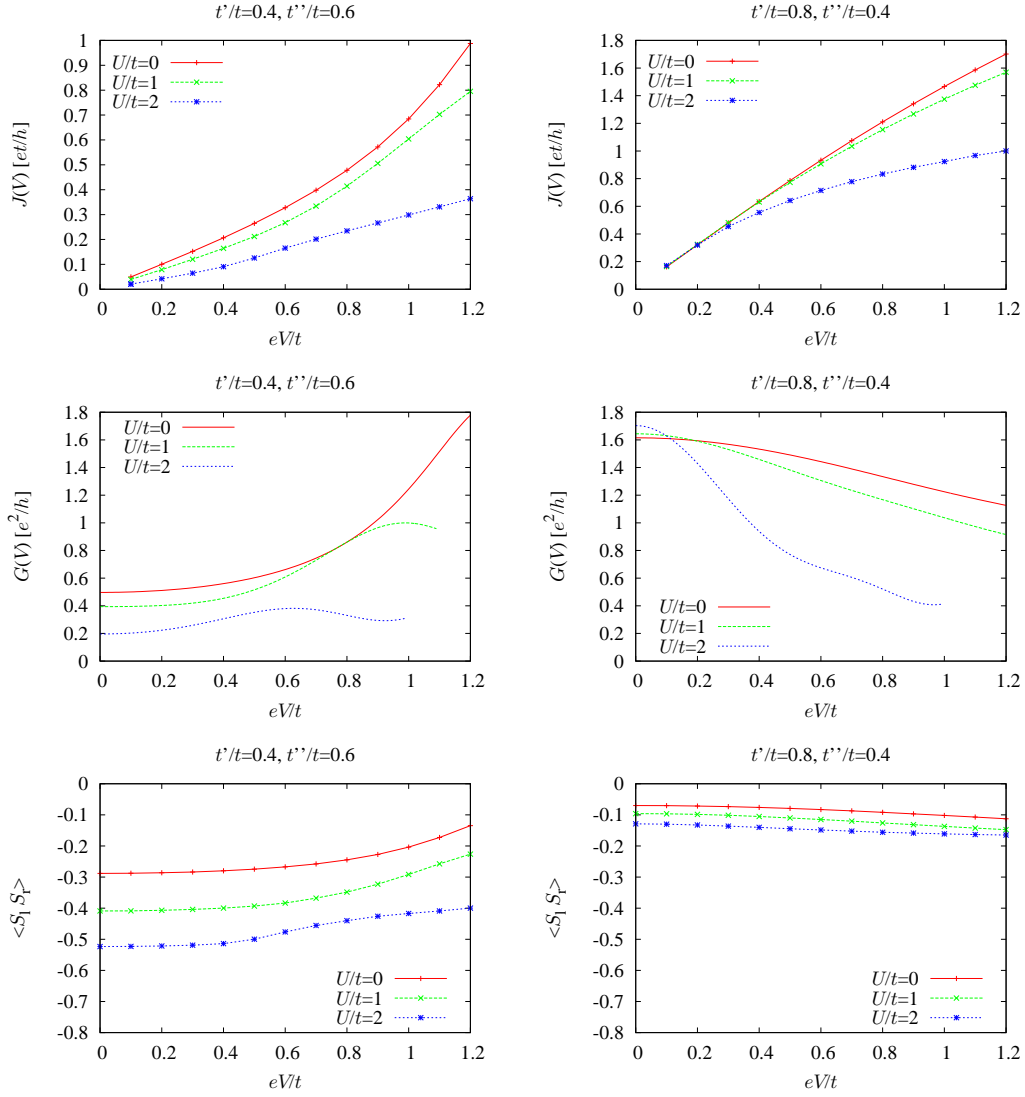


Fig. 6 Current-voltage characteristics $J(V)$, differential conductance $G(V)$ and the expectation values of the spin correlation function $\langle \vec{S}_l \cdot \vec{S}_r \rangle$ for $(t'/t, t''/t) = (0.4, 0.6)$ and $(0.8, 0.4)$. The TdDMRG calculations have been performed for the systems with $L = 121$.

dots, the interdot coherence seems to be partly recovered. This does not conform to a naive expectation that the finite bias voltage suppresses the electron correlation effects in a similar way as the finite temperature does. This enhancement of the interdot correlation by the voltage has similarity to the suppression of the double occupancy $\langle n_{\text{dot}\uparrow} n_{\text{dot}\downarrow} \rangle$ by the voltage in the single quantum dot system [9, 24].

4 Conclusions

In this paper we have reviewed recent developments on the TdDMRG method applied to the nonequilibrium transport through quantum dots. The results for a single dot show clearly that one can obtain reliable results on steady currents in systems with correlation effects up to the intermediate coupling regime.

In the second part of this paper, we have investigated the nonlinear transport through serially coupled double-quantum-dot system. We have accurately simulated the quasi-steady states and discussed how the steady currents are affected by the competition between the formation of the two-Kondo singlets (the state (i)) and the local singlet states (the pair spin singlet (ii) and the doubly occupied bonding singlet (iii)).

It has been found that the differential conductance shows splitting of the zero bias peak when the ground state is of the local nature, namely near the state (ii) or (iii). The positions of the split peaks in the differential conductance are renormalized to smaller values towards 0 as U increases under the condition of the particle-hole symmetry. In addition we have shown that in the cases near the state (i) the interdot spin correlation can be enhanced by applying a finite voltage.

The results presented in this paper indicate that it is now possible to perform unbiased numerical calculations for nonequilibrium steady states of strongly correlated electron systems. The approach based on the TdDMRG is from one-dimension and of course a complementary approach is from higher dimensions, notably from the infinite dimension.

Acknowledgements It is our great pleasure to dedicate the present paper to Professor Vollhardt for his sixtieth birthday. This work was supported by JSPS Grant-in-Aid for JSPS Fellows 21-6752, by Grant-in-Aid on Innovative Areas “Heavy Electrons” (No. 20102008) and also by Scientific Research (C) (No. 20540347). S. K. is supported by the Japan Society for the Promotion of Science.

References

- [1] T. K. Ng and P. A. Lee, Phys. Rev. Lett. **61**, 1768 (1988); L. I. Glazman and M. E. Raikh, Zh. Éksp. Teor. Fiz. **47**, 378 (1988) [JETP Lett. **47**, 452 (1988)].
- [2] D. Goldhaber-Gordon, H. Shtrikman, D. Mahalu, D. Abusch-Magder, U. Meirav and M. A. Kastner, Nature (London) **391**, 156 (1998); D. Goldhaber-Gordon, J. Göres, M. A. Kastner, H. Shtrikman, D. Mahalu and U. Meirav, Phys. Rev. Lett. **81**, 5225 (1998); S. M. Cronenwett, T. H. Oosterkamp and L. P. Kouwenhoven, Science **281**, 540 (1998); W. G. van der Wiel, S. De Franceschi, T. Fujisawa, J. M. Elzerman, S. Tarucha and L. P. Kouwenhoven, Science **289**, 2105 (2000).
- [3] W. Metzner and D. Vollhardt, Phys. Rev. Lett. **62**, 324 (1989).
- [4] A. Georges, G. Kotliar, W. Krauth and M. J. Rozenberg, Rev. Mod. Phys. **68**, 13 (1996).
- [5] S. R. White, Phys. Rev. Lett. **69**, 2863 (1992); S. R. White, Phys. Rev. B **48**, 10345 (1993).
- [6] A. J. Daley, C. Kollath, U. Schollwöck and G. Vidal, J. Stat. Mech., Theor. Exp. P04005 (2004); S. R. White and A. Feiguin, Phys. Rev. Lett. **93**, 076401 (2004).
- [7] See J. Eckel, F. Heidrich-Meisner, S. G. Jakobs, M. Thorwart, M. Pletyukhov and R. Egger, New J. Phys. **12** 043042 (2010) and references therein.
- [8] K. A. Al-Hassanieh, A. E. Feiguin, J. A. Riera, C. A. Büsser and E. Dagotto, Phys. Rev. B **73** 195304 (2006).
- [9] S. Kirino, J. Zhao, T. Fujii and K. Ueda, J. Phys. Soc. Jpn. **77**, 084704 (2008).
- [10] F. Heidrich-Meisner, A. E. Feiguin and E. Dagotto, PRB **79** 235336 (2009).
- [11] S. Kirino, T. Fujii and K. Ueda, Physica E **42**, 874 (2010).
- [12] E. Boulat, H. Saleur and P. Schmitteckert, Phys. Rev. Lett. **101** 140601 (2008).
- [13] A. Branschädel, G. Schneider and Peter Schmitteckert, Ann. Phys. **522** 657 (2010).
- [14] S. Hershfield, J. H. Davies and J.W. Wilkins, Phys. Rev. Lett. **67**, 3720 (1991); Phys. Rev. B **46**, 7046 (1992).
- [15] T. H. Oosterkamp, T. Fujisawa, W. G. van der Wiel, K. Ishibashi, R. V. Hijman, S. Tarucha and L. P. Kouwenhoven, Nature **395**, 873 (1998).
- [16] T. Fujisawa, T. H. Oosterkamp, W. G. van der Wiel, B. W. Broer, R. Aguado, S. Tarucha and L. P. Kouwenhoven, Science **282**, 932 (1998).
- [17] H. Jeong, A. M. Chang and M. R. Melloch, Science **293**, 2221 (2001).
- [18] W. G. van der Wiel, S. De Franceschi, J. M. Elzerman, T. Fujisawa, S. Tarucha and L. P. Kouwenhoven, Rev. Mod. Phys. **75**, 1 (2002), and references therein.
- [19] A. Georges and Y. Meir, Phys. Rev. Lett. **26**, 3508 (1999).
- [20] T. Aono, M. Eto and K. Kawamura, J. Phys. Soc. Jpn. **67**, 1860 (1998); T. Aono and M. Eto, Phys. Rev. B **63**, 125327 (2001).
- [21] W. Izumida and O. Sakai, Phys. Rev. B **62**, 10260 (2000); W. Izumida and O. Sakai, J. Phys. Soc. Jpn. **74**, 103 (2005).
- [22] Y. Meir and N. Wingreen, Phys. Rev. Lett. **68**, 2512 (1992).
- [23] For a complete set of data see, S. Kirino, Ph. D. thesis, The University of Tokyo (2011).
- [24] P. Werner, T. Oka and A. J. Mills, Phys. Rev. B **79** 035320 (2009).